

Theory of Two-Photon Spectroscopy in Solids*

G. D. MAHAN†

*Institute of Theoretical Science and Department of Physics, University of Oregon, Eugene, Oregon and
General Electric Research and Development Center, Schenectady, New York*

(Received 2 January 1968)

The coefficient of absorption of two photons is calculated for a two-band model of a solid. The frequency and polarization dependence is evaluated for the case that one photon (laser) frequency is fixed while the second is varied. Wannier exciton states are explicitly included in both the intermediate and final states. Depending upon the symmetry of the two energy bands, the final state may either be an exciton s , p , or d state. All three cases have different frequency and polarization dependences. The final formulas for the matrix element are complicated, and approximate formulas are given which are useful for many applications. It is shown that some of the two-photon spectroscopy experiments in semiconductors and alkali halides which have been reported so far can be explained by these calculations.

I. INTRODUCTION

TWO-PHOTON spectroscopy is emerging as a useful complement to one-photon optics in solid-state physics. In two-photon experiments, the electronic state changes its energy by the sum of the two photon energies, and the solid does not absorb at either of the individual frequencies. If one of the photons is from a laser, so that its energy is fixed, the other photon frequency can be varied to obtain a spectrum. In order to prevent the absorption of two laser photons, the laser energy is selected to be less than half of the energy gap of the insulator which is being studied. Since the pioneering experiment of Hopfield and Worlock¹ on KI and CsI, these measurements have been performed on other alkali halides,² TiCl₃,³ CdS,⁴ ZnS,⁴ CuCl,⁵ and anthracene.⁶

There have been several theoretical calculations of two-photon absorption.⁷⁻¹¹ In most of these,⁷⁻¹⁰ a three-band model is assumed for the solid. The absorption of the first photon lifts an electron from the valence band to a virtual state in some higher-lying conduction band. The absorption of the second photon takes the electron to its final state in another conduction band. The conduction band which serves as an intermediate state is usually considered to be at a higher energy than

the final state, which has experimentally been the direct conduction band. Another three-band process worth mentioning involves a lower valence band as an intermediate state. Here the first photon takes an electron from a deep valence band to the final conduction band. The second photon fills this deep-valence-band hole with an electron from the top valence band.

Louden⁹ pointed out that the electronic transition must produce an exciton state. If symmetry allows all of the interband matrix elements, then, as in the one-photon transition, the absorption coefficient is proportional to $|\psi_\lambda(r=0)|^2$, where ψ_λ is the hydrogenic relative wave function of the exciton. The $|\psi_\lambda(0)|^2$ behavior strongly influences the character of the absorption coefficient at the interband threshold. Loudon's approach has been adopted in most subsequent theoretical discussions.

First we note that one does not need to include three bands in discussing the two-photon absorption. Instead, one can discuss the process entirely within a two-band model.^{1,11} The first photon creates a virtual exciton composed of electrons and holes from these two bands. The second photon changes the system from the intermediate exciton state to the final exciton state. In both the two- and three-band models the final state is an exciton. In our calculations for the two-band model we also include exciton effect in the intermediate state. Exciton effects in the intermediate state have been omitted from previous calculations using the three-band model, and this may affect the accuracy of these calculations.

The present investigation calculates two-photon absorption using the two-band model. Transitions which occur in real solids will reach the final state by using every path through every intermediate which is available. Whether the important process involves two bands, three bands, or any other path, depends upon the parameters of the material. We feel that the two-band process is an important one, and deserving of consideration. Furthermore, in Sec. IV, where we compare our results to the experiments, we show that many of the past two-photon experiments can be explained by the two-band model.

* Research supported by the National Science Foundation.

† Present address: Institute of Theoretical Science, University of Oregon, Eugene, Ore. 97403.

¹ J. J. Hopfield and J. M. Worlock, *Phys. Rev.* **137**, A1455 (1965); J. J. Hopfield, J. M. Worlock, and K. Park, *Phys. Rev. Letters* **11**, 414 (1963).

² D. Fröhlich and B. Stagginnus, *Phys. Rev. Letters* **19**, 496 (1967).

³ M. Matsuoka and T. Yajima, *Phys. Letters* **23**, 54 (1966); M. Matsuoka, *J. Phys. Soc. Japan*, **23**, 1028 (1967).

⁴ P. J. Regensburger and E. Panizza, *Phys. Rev. Letters* **18**, 113 (1967); E. Panizza, *Appl. Phys. Letters* **10**, 265 (1967).

⁵ D. Fröhlich, B. Stagginnus, and E. Schonherr, *Phys. Rev. Letters* **19**, 1032 (1967).

⁶ D. Fröhlich and H. Mahr, *Phys. Rev. Letters* **16**, 895 (1966).

⁷ D. Kleinman, *Phys. Rev.* **125**, 87 (1962).

⁸ R. Braunstein, *Phys. Rev.* **125**, 475 (1962); R. Braunstein and N. Ockman, *ibid.* **134**, A499 (1964).

⁹ R. Loudon, *Proc. Roy. Soc. (London)* **80**, 952 (1962).

¹⁰ M. Inoue and Y. Toyozawa, *J. Phys. Soc. Japan* **20**, 363 (1965).

¹¹ G. D. Mahan, Ph.D. thesis, University of California, 1964 (unpublished).

The two-band and three-band models not only differ in the number of bands involved in the excitation process, but they also predict different spectral dependences for the absorption coefficient. In the two-band model, the final exciton may be in an s , p , or d state. Indeed, in some of the experiments which have been done, all three types were probably being excited. The spectral dependences of s , p , and d excitons are all quite different. They also have different dependences upon the angle of polarization of the photons.

Even for s -state excitons, the two-band and three-band models predict different spectral shapes. In the two-band case, the absorption coefficient is *not* just proportional to $|\psi_n(0)|^2$. The actual absorption coefficient has a far more complicated dependence upon the hydrogenic quantum number n .

The absorption coefficients for s , p , and d states are calculated in Secs. II and III. The actual results are mathematically complicated. In fact, the actual matrix element requires a simple computer program for exact evaluation. In order to make the results more useful, some approximate formulas are presented which are reasonably accurate in some cases. In fact, these approximate formulas were given earlier.¹¹ The important parameter is

$$\kappa_\alpha = E_B / (E_G - \hbar\omega_\alpha),$$

where E_B and E_G are the exciton binding energy and the direct interband energy gap, respectively. There are two values of κ_α in the problem, one for each photon energy ($\hbar\omega_1$ and $\hbar\omega_2$ give κ_1, κ_2). If both values of κ_α are "small" ($\kappa_\alpha \leq 0.2$), the approximate formulas work quite well. When κ_α is "large" ($\kappa_\alpha \simeq 0.5$), the approximate formulas adequately give the magnitude of the absorption, but are poor for predicting the shape.

Inoue and Toyozawa¹⁰ pointed out the complicated polarization dependence of exciton s -state absorption in two-photon spectroscopy. Since each transition with a different type of group symmetry has a unique polarization dependence, this enables one to experimentally deduce the particular transition involved. This important idea has already been exploited by Frohlich *et al.* in studying CuCl.⁵ This polarization dependence, which can be deduced from group-theoretical arguments, is the same for the two-band and three-band models. We have calculated the polarization dependence of p and d exciton states for cubic crystals. Our calculation of the polarization dependence of p states explained the dependence which was observed in the alkali halides.¹² An extended comparison between theory and experiment is given in Sec. IV.

II. ALLOWED DIPOLE TRANSITIONS: p -STATE EXCITONS

First we consider the case where the conduction-band to valence-band dipole transition is allowed. In cubic

crystals in which parity is a valid concept, the absorption of two photons requires the initial and final electronic states to have the same parity. The allowed conduction-band to valence-band transition involves a parity change. Therefore, the final Wannier exciton state must have odd parity in order to keep the parity change even. As will be shown below, the final exciton is in a p state.

The basic transition probability for the two-quantum process is

$$W = \frac{2\pi}{\hbar} \sum_{if} S_f(E) |V_{if}|^2, \quad (2.1)$$

where S_f is the final density of states. We take $\hbar\omega_1$ to be the fixed laser energy, while $\hbar\omega_2$ is the variable second frequency. The matrix element V_{if} between the initial and final states is

$$V_{fi} = \frac{e^2}{m^2 c^2} A(1)A(2) \sum_i \left[\frac{\langle f | \hat{\epsilon}_1 \cdot \mathbf{p} | l \rangle \langle l | \hat{\epsilon}_2 \cdot \mathbf{p} | i \rangle}{E_l - E_i - \hbar\omega_2} + \frac{\langle f | \hat{\epsilon}_2 \cdot \mathbf{p} | l \rangle \langle l | \hat{\epsilon}_1 \cdot \mathbf{p} | i \rangle}{E_l - E_i - \hbar\omega_1} \right], \quad (2.2)$$

where $A(1)$ is the vector potential for photons $\hbar\omega_1$, and $\hat{\epsilon}_1$ is the polarization vector. For this two-step process, we have included the sum over intermediate states $|l\rangle$ of energy E_l . After we have evaluated (2.2) and (2.1) we will wish to calculate the attenuation constant α_2 of the second optical beam

$$\alpha_2 = 2(W n_2 / c N_2), \quad (2.3)$$

where n_2 and N_2 are the refraction index and number density of the photon $\hbar\omega_2$. The attenuation constant α_2 will be proportional to the power $P_1 = N_1 \hbar\omega_1 c / V n_1$ in the laser beam.

The two kinds of matrix elements which enter (2.2) are easy to evaluate. It is the sum over intermediate states which makes the calculation difficult. The initial state has no excitons, and we set $E_i = 0$. The intermediate states are exciton states with $E = E_G + E_{n,0}$. $E_{n,0}$ is the exciton energy for hydrogenic state n . The exciton center-of-mass wave vector is set equal to zero since it is just of the order of the photon wave vectors. The first matrix element is evaluated following the procedure outlined by Elliott.¹³

$$\langle l | \hat{\epsilon}_\alpha \cdot \mathbf{p} | i \rangle = \sqrt{V} \psi_\lambda^*(0) \langle c | \hat{\epsilon}_\alpha \cdot \mathbf{p} | v \rangle. \quad (2.4)$$

The relative wave function $\psi_\lambda(0)$ is evaluated at $r=0$, and the matrix element $\langle c | \hat{p} | v \rangle$ is evaluated between Bloch functions. We assume that the exciton states are of the Wannier type. The absorption of the second photon changes the exciton states, and the second matrix element reduces to an integral between exciton

¹² G. D. Mahan, Phys. Rev. Letters **20**, 332 (1968).

¹³ R. J. Elliott, Phys. Rev. **108**, 1384 (1957).

hydrogenic wave functions:

$$\frac{1}{m} \langle f | \hat{\epsilon}_\beta \cdot \mathbf{p} | l \rangle = \frac{1}{\bar{\mu}} \int d^3r \psi_\delta^*(r) \hat{\epsilon}_\beta \cdot \mathbf{p} \psi_\lambda(r). \quad (2.5)$$

The quantum numbers δ for the final states are (n, l, m) for bound states, and \mathbf{k} for continuum states. The exciton reduced mass is $\bar{\mu}$.

At this point it is convenient to define a special symbol for the sum over intermediate states:

$$I_\delta(\alpha, \beta) = \int d^3r \psi_\delta^*(r) \hat{\epsilon}_\beta \cdot \mathbf{p} \sum_\lambda \frac{\psi_\lambda(r) \psi_\lambda^*(0)}{E_{\lambda,0} + E_G - \hbar\omega_\alpha}. \quad (2.6)$$

The symbols α and β can be 1 or 2 for the two photons $\hbar\omega_1$ and $\hbar\omega_2$. Our general matrix element (2.2) is

$$V_{fi} = \frac{\sqrt{V} e^2}{\bar{\mu} m c^2} A(1) A(2) \times [\langle c | \hat{\epsilon}_1 \cdot \mathbf{p} | v \rangle I_\delta(1, 2) + \langle c | \hat{\epsilon}_2 \cdot \mathbf{p} | v \rangle I_\delta(2, 1)]. \quad (2.7)$$

In order to evaluate the integral (2.6), we note that the sum over λ is just the Coulomb Green's function

$$G(r, r') = \sum_\lambda \frac{\psi_\lambda(r) \psi_\lambda^*(r')}{E_\lambda - \Omega},$$

where E_λ is the exciton hydrogenic energy as measured from the conduction-band edge. For the case (2.6) with $r' = 0$ and $\Omega = -E_G + \hbar\omega_\alpha < 0$, this can be expressed as a Whittaker's function¹⁴:

$$G(r, 0) = (\bar{\mu}/2\pi r \hbar^2) \Gamma(1-\kappa) W_{\kappa, 1/2}(2r/a\kappa) \quad (2.8)$$

$$\kappa_\alpha = [E_B/(E_G - \hbar\omega_\alpha)]^{1/2}.$$

The subscript α or β on κ is omitted in (2.8), but κ means either κ_1 or κ_2 for $\alpha = 1, 2$. The exciton Bohr radius is a and reduced mass is $\bar{\mu}$. Since we assume that the hydrogenic Wannier exciton states are isotropic in space, then $G(r, 0)$ only depends upon the magnitude of r . Hence

$$\hat{\epsilon}_\beta \cdot \mathbf{p} G(r, 0) = -i\hbar \hat{\epsilon}_\beta \cdot \hat{r} (\partial/\partial r) G(r, 0).$$

Thus, the sum over intermediate states in (2.6) becomes

$$I_\delta(\alpha, \beta) = -i\hbar \int d^3r \psi_\delta^*(r) \hat{\epsilon}_\beta \cdot \hat{r} \frac{\partial}{\partial r} G(r, 0). \quad (2.9)$$

It is obvious from (2.9) that the final state ψ_δ must be a p state. However in order to make further progress in evaluating (2.9), we must separately treat the cases where ψ is a bound or a continuum exciton state.

¹⁴ L. Hostler, J. Math. Phys. 5, 591 (1964).

A. p -Exciton Bound States

The bound states of the exciton are given by the usual Coulomb wave functions¹⁵

$$\psi_{nlm} = \frac{Y_{l,m}(\theta, \varphi) 2}{a^{3/2} n^2 (2l+1)!} \left[\frac{(n+l)!}{(n-l-1)!} \right]^{1/2} \times \rho^l e^{-\rho/2} F_1(1+l-n, 2l+2, \rho), \quad (2.10)$$

$$\rho = 2r/an.$$

The $Y_{l,m}$ are the usual spherical harmonic functions. Since we have assumed spherical symmetry, we can quantize the exciton Hamiltonian in any convenient direction. If one chose the $\hat{\epsilon}_\beta$ direction, the final state is $l=1, m=0$, and the angular integral in (2.9) gives

$$\int d\Omega Y_{1,0}(\theta, \varphi) \hat{\epsilon}_\beta \cdot \hat{r} = (\frac{4}{3}\pi)^{1/2}.$$

The derivative $(\partial/\partial r)G(r, 0)$ is easily performed by using the following representation for the Whittaker's function¹⁶

$$W_{\kappa, 1/2}(z) = \frac{ze^{-z/2}}{\Gamma(1-\kappa)} \int_0^\infty dt e^{-zt} \left(\frac{1+t}{t} \right)^\kappa. \quad (2.11)$$

Furthermore, the r integral in (2.9) can be performed by using¹⁷

$$\int_0^\infty d\rho \rho^{\sigma-1} e^{-\rho p} {}_1F_1(\alpha; \sigma; \lambda\rho) = \Gamma(\sigma) p^{\alpha-\sigma} / (p-\lambda)^\alpha. \quad (2.12)$$

After performing these operations, the integral in (2.9) becomes the somewhat more simplified result

$$I_{n, l=1}(\alpha, \beta) = \hbar / [iE_B(3\pi a^5)^{1/2}] \times [(n^2-1)/n^5]^{1/2} J_{p,n}(\kappa_\alpha) \quad (2.13)$$

$$J_{p,n}(\kappa) = \frac{\kappa^2}{2} \int_0^\infty dt \times (t+\frac{1}{2}) \left(\frac{1+t}{t} \right)^\kappa \frac{[t+\frac{1}{2}-\kappa/2n]^{n-2}}{[t+\frac{1}{2}+\kappa/2n]^{n+2}}. \quad (2.14)$$

The $J_{p,n}$ integration in (2.14) can not be performed in a simple analytical fashion. About the best one can do is to numerically integrate; or else express (2.14) as a double series. Some of these methods are discussed in the Appendix I. There it is shown that one way of

¹⁵ L. Schiff, *Quantum Mechanics* (McGraw-Hill Book Co., New York, 1949).

¹⁶ *Handbook of Mathematical Functions*, edited by M. Abramowitz and I. A. Stegun (U. S. Department of Commerce, National Bureau of Standards, Washington, D. C., 1964), Appl. Math. Ser. 55.

¹⁷ *Tables of Integral Transforms*, edited by A. Erdelyi (McGraw-Hill Book Co., New York, 1954), Vol. I, p. 217.

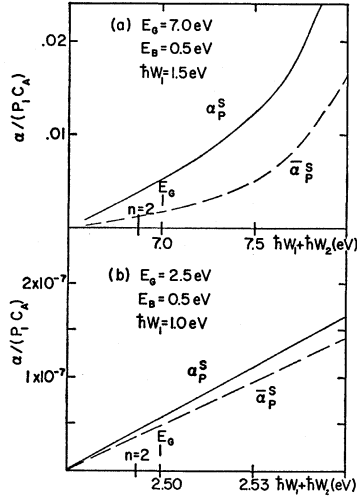


FIG. 1. The two-photon absorption coefficient for exciton p states calculated from the exact (α_p^S) and approximate ($\bar{\alpha}_p^S$) equations. In part (a) the parameters are characteristic of an alkali halide. Here the values of κ are large (~ 0.5) and the approximate expression does not resemble the exact result. In part (b) the parameters are characteristic of a semiconductor with a small binding energy. Here the values of κ are small (~ 0.15) and the approximate formulas work reasonably well. At low temperatures, the absorption will start abruptly in the vicinity of the $n=2$ exciton line. The superscript S means that the two photons were polarized in the same direction. *Note added in proof.* In part (b), the value for E_B is given incorrectly, and should be $E_B=0.03$ eV.

evaluating (2.14) is

$$J_{p,n}(\kappa) = \frac{\Gamma(1-\kappa)\kappa^2}{2t_0^{2+\kappa}} \sum_{l=0}^{n-2} \frac{(2-n)_l}{l!} \left(\frac{\kappa}{nt_0}\right)^l \times \left[\frac{\Gamma(l+2)}{\Gamma(l+3-\kappa)} {}_2F_1(1-\kappa, -\kappa; l+3-\kappa; 1-t_0) - \frac{\kappa}{2t_0n} \times \frac{\Gamma(l+3)}{\Gamma(l+4-\kappa)} {}_2F_1(1-\kappa, -\kappa; l+4-\kappa; 1-t_0) \right], \quad (2.15)$$

where

$$t_0 = \frac{1}{2}(1 + \kappa/n), \quad (2.16)$$

and ${}_2F_1$ is the standard hypergeometric function. This result, although somewhat complicated, has two interesting features. First, the transition probability to the lowest exciton states is easily evaluated since the sum over l contain just a few terms. For example, to the first p state at $n=2$, there is just the one term in the sum ($l=0$)

$$J_{p,2}(\kappa) = \frac{\Gamma(1-\kappa)\kappa^2}{\Gamma(3-\kappa)2t_0^{2+\kappa}} \left[{}_2F_1(1-\kappa, -\kappa; 3-\kappa, 1-t_0) - \frac{\kappa}{t_0n(3-\kappa)} {}_2F_1(1-\kappa, -\kappa; 4-\kappa, 1-t_0) \right].$$

Since ${}_2F_1$ is a series, (2.15) is basically a double series. The second useful feature of (2.15) is that both of these

series converge for the physically interesting domain of $\kappa/n < 1$. In fact, (2.15) was used in the numerical calculations described below.

Now that the matrix element has been evaluated, we can evaluate the absorption coefficient. We must also specify the angular dependence of the absorption coefficient. In cubic materials, the matrix element $\langle c | \hat{\epsilon}_\alpha \cdot \mathbf{p} | v \rangle$ requires that the conduction and valence band symmetries differ by T_{1u} . Thus there is only one kind of polarization dependence which is common to all different possible initial and final states.

Each combination of Bloch functions which have the symmetry T_{1u^x} , T_{1u^y} , T_{1u^z} are different final states. One also gets different final states for the three hydrogenic wave functions which transform like (x, y, z) . When one includes all of these possibilities, one gets an effective matrix element of

$$J_{\text{eff},n}^2 = \frac{1}{2}(\hat{\epsilon}_1 \times \hat{\epsilon}_2)^2 |J_{p,n}(\kappa_1) - J_{p,n}(\kappa_2)|^2 + \frac{1}{2}[1 + (\hat{\epsilon}_1 \cdot \hat{\epsilon}_2)^2] |J_{p,n}(\kappa_1) + J_{p,n}(\kappa_2)|^2 = \cos^2\theta |J_{p,n}(\kappa_1) + J_{p,n}(\kappa_2)|^2 + \sin^2\theta [J_{p,n}(\kappa_1)^2 + J_{p,n}(\kappa_2)^2], \quad (2.17)$$

where θ is the angle between $\hat{\epsilon}_1$ and $\hat{\epsilon}_2$.

This form is actually quite simple to understand. The two terms $J_{p,n}(\kappa_1)$ and $J_{p,n}(\kappa_2)$ arise from the two terms in (2.7)—i.e., the two photons may be absorbed in either order. If the two polarizations $\hat{\epsilon}_1$ and $\hat{\epsilon}_2$ are parallel ($\cos^2\theta=1$), both terms create the same final state. Here one must add the two terms before squaring the matrix element. When the two polarizations $\hat{\epsilon}_1$ and $\hat{\epsilon}_2$ are perpendicular ($\sin^2\theta=1$), each of the two terms in (2.7) creates a different final state (although the two states are degenerate). Here one squares the matrix elements before adding. The general result (2.17) provides the correct interpolation between these extremes.

After collecting our result (2.1), (2.3), (2.7), (2.13), and (2.17), the absorption coefficient for a particular exciton state of $n, l=1$ is

$$\alpha_p = P_1 C_A \frac{S_n 2E_B}{n^3} \frac{E_B}{\hbar^3 \omega_1^2 \omega_2} (1 - 1/n^2) J_{\text{eff},n}^2 \quad (2.18a)$$

$$C_A = \frac{32\pi^2}{n_1 n_2} \left(\frac{e^2}{\hbar c}\right)^2 \frac{\hbar^3 |\langle c | p_x | v \rangle|^2}{am^2 E_B^4 \omega_1^2}. \quad (2.18b)$$

We have tried to collect in (2.18b) all of the factors which are independent of frequency. This choice is somewhat arbitrary, since the refractive index n_2 and the matrix element $\langle c | p | v \rangle$ will both vary as $\hbar\omega_2$ is varied. However, for the present discussion, we will treat C_A as a constant.

For a sharp, well-defined exciton line, the density of states S_n will have a Lorentzian character. These sharp lines are only experimentally observed for the lowest values of n . For higher values of n in the exciton bound-state spectrum, the lines are broad and they overlap, which causes a smooth spectra. Then one takes S_n to

be $n^3/2E_B$. Here one also treats n as a continuous variable,

$$-1/n^2 = \Delta = (\hbar\omega_1 + \hbar\omega_2 - E_G)/E_B.$$

In this case, the absorption coefficient (2.17) is

$$\alpha_p = P_1 C_A (E_B^3 / \hbar^3 \omega_1^2 \omega_2) (1 + \Delta) J_{\text{eff}, n^2}. \quad (2.19)$$

When evaluating $J_{p,n}(\kappa)$ in (2.15), n can be treated as a noninteger number by letting the sum over l extend to infinity. Some examples of the absorption coefficient (2.19) are given in Fig. 1.

B. p -Exciton Continuum States

When the sum of the two photon energies exceeds the energy gap, the exciton states are no longer bound. Here one pictures the electron and hole in a relative scattering state. The Coulomb wave functions are¹⁵

$$\begin{aligned} \psi(\mathbf{k}, \mathbf{r}) &= \frac{e^{\eta\pi/2}}{\sqrt{V}} \sum_{l=0}^{\infty} \frac{|\Gamma(l+1-i\eta)|}{(2l)!} (i\rho)^l e^{i\rho l/2} \\ &\times P_l(\cos\omega) {}_1F_1(l+1-i\eta, 2l+2, -i\rho). \quad (2.20) \end{aligned}$$

When we put this wave function in (2.9), the angular integrals must be treated carefully. Both \mathbf{k} and \mathbf{r} can point in any direction, and $\cos\omega$ is the angle between them. If $\hat{\epsilon}_\beta = \hat{z}$, and $\mathbf{r} = (r, \theta, \varphi)$, and $\mathbf{k} = (k, \theta_0, \varphi_0)$ in spherical coordinates, then

$$\int \frac{d\Omega}{4\pi} \hat{\epsilon}_\beta \cdot \hat{r} P_l(\cos\omega) = \cos\theta_0 = \frac{k_z}{k}. \quad (2.21)$$

The r integral in (2.9) is evaluated for continuum states by following the procedure for bound states. One uses (2.11) and (2.12), and gets

$$I_{k,l=1}(\alpha, \beta) = \frac{\hbar e^{\eta\pi/2} |\Gamma(2-i\eta)| J_{p,k}(\kappa_\alpha)(\mathbf{k} \cdot \hat{\epsilon}_\beta)}{\sqrt{V E_B}}, \quad (2.22)$$

$$\begin{aligned} J_{p,k}(\kappa) &= \frac{\kappa^2}{2} \int_0^\infty dt \left(\frac{1+t}{t} \right)^\kappa \left(t + \frac{1}{2} \right) \\ &\times [t + \frac{1}{2} - i\kappa/2\eta]^{-(2+i\eta)} \\ &\times [t + \frac{1}{2} + i\kappa/2\eta]^{-(2-i\eta)}. \quad (2.23) \end{aligned}$$

When we compare the two integrals (2.14) and (2.23) we see that $n \rightarrow i\eta$ in going from the bound-state result (2.13) to the continuum result (2.23). Therefore, it can also be shown that (2.23) can also be expressed as a double series like (2.15), except with $n \rightarrow i\eta$. In this case the terms are all complex, and this makes the series inconvenient to evaluate. Although the terms in this series are complex, their sum $J_{p,k}(\kappa)$ is real. This is because the integral (2.23) is real, since the complex terms are conjugates of each other:

$$\begin{aligned} &[t + \frac{1}{2} - i\kappa/2\eta]^{-(2+i\eta)} [t + \frac{1}{2} + i\kappa/2\eta]^{-(2-i\eta)} \\ &= \frac{\exp\{-2\eta \tan^{-1}[\kappa/\eta(2t+1)]\}}{[(t + \frac{1}{2})^2 + (\kappa/2\eta)^2]^2}. \end{aligned}$$

We have evaluated this integral by direct numerical integration. After changing variables $S = (2t+1)^{-1}$, we get

$$\begin{aligned} J_{p,k}(\kappa) &= 2\kappa^2 \int_0^1 dS \frac{S^{[\kappa(1+S)/(1-S)]}}{[1+(S\kappa/\eta)^2]^2} \\ &\times \exp\{-2\eta \tan^{-1}(S\kappa/\eta)\}. \quad (2.24) \end{aligned}$$

This integral is straightforward to evaluate numerically. The integrand diverges at $S \rightarrow 1$, but this divergence is integrable for $\kappa < 1$. Actually, one could also evaluate (2.14) by using an integral like (2.24), and this may even be faster than using (2.15).

Since the matrix element has been evaluated, it is now simple to calculate the absorption coefficient. The sum over final density of states is

$$\sum_f S_f = \frac{2V}{(2\pi)^3} \int d^3k \delta\left(\hbar\omega_1 + \hbar\omega_2 - E_G - \frac{\hbar^2 k^2}{2\mu}\right). \quad (2.25)$$

When we evaluate the angular integrals in (2.25), a $\frac{1}{3}$ factor arises from the $\cos^2\theta_0$ term which comes from the square of (2.21). A similar $\frac{1}{3}$ factor arises in one-photon absorption when the conduction to valence-band dipole moment is forbidden. Most derivations of the one-photon case do not explicitly include the k_z dependence of the matrix element, yet they manage to somehow include the $\frac{1}{3}$ factor later in the calculation. However, the present method is correct, and it is especially important to do this properly when discussing d -state absorption.

The absorption coefficient is

$$\alpha_p = P_1 \frac{C_A E_B^3}{\hbar^3 \omega_1^2 \omega_2} (1 - e^{-2\eta\pi})^{-1} (1 + 1/\eta^2) J_{\text{eff}, k^2}. \quad (2.26)$$

The matrix element J_{eff, k^2} in (2.26) is the same as (2.17) except with $J_{p,k}$ instead of $J_{p,n}$. The C_A in (2.26) is given in (2.18). The result (2.26) is very similar to the absorption coefficient (2.19) for the higher bound states. In (2.26), we have

$$1/\eta^2 = \Delta = (\hbar\omega_1 + \hbar\omega_2 - E_G)/E_B, \quad (2.26')$$

which will make (2.26) resemble (2.19) even more closely. In fact, the absorption from the bound state (2.19) and continuum states (2.26) is continuous at the energy gap. This is demonstrated by showing that $J_{p,n}$ and $J_{p,k}$ have the same value at $\Delta = 0$,

$$\begin{aligned} \lim_{n \rightarrow \infty} J_{p,n}(\kappa) &= \lim_{k \rightarrow 0} J_{p,k}(\kappa) = \kappa^2 2^{1+\kappa} \sum_{l=0}^{\infty} \frac{(-2\kappa)^l (l+1)}{\Gamma(3+l-\kappa)} \\ &\times {}_2F_1(1-\kappa, -\kappa, l+3-\kappa, 1-t_0). \quad (2.27) \end{aligned}$$

This continuity of the absorption spectra at the energy gap is also characteristic of the one-photon absorption spectra.

C. Approximate Solution

The absorption coefficients which have been derived require numerical computation to be evaluated correctly. It would be extremely convenient to have approximate formulas for $J_{p,n}(\kappa)$ and $J_{p,k}(\kappa)$. These simplifications exist for some range of the parameters—in particular, when κ_1 and κ_2 are small.

In the series expansion (2.15) for $J_{p,n}(\kappa)$, the first correction terms are of the order of κ . If κ is small, these higher terms may be neglected. It was noted that $J_{p,k}(\kappa)$ can be expanded in a similar series, and here the first correction terms are also smaller by a factor of κ .

$$\begin{aligned} J_{p,n}(\kappa) &= \kappa^2 [1 + O(\kappa)] \\ J_{p,k}(\kappa) &= \kappa^2 [1 + O(\kappa)]. \end{aligned} \quad (2.28)$$

Using these approximate expressions for $J_{p,n}$ and $J_{p,k}$, the absorption coefficient for $\hat{\epsilon}_1 \parallel \hat{\epsilon}_2$ is

$$\bar{\alpha}_p = P_1 C_A \frac{E_B^3}{\hbar^3 \omega_1^2 \omega_2} [1 + \Delta] [\kappa_1^2 + \kappa_2^2]^2 T(\Delta), \quad (2.29)$$

where

$$\begin{aligned} T(\Delta) &= S_n 2E_B/n^3 \text{ for discrete exciton states,} \\ T(\Delta) &= 1 \text{ for the closely spaced bound states, } \Delta < 0, \\ T(\Delta) &= (1 - e^{-2\pi/\sqrt{\Delta}})^{-1} \text{ for } \Delta > 0. \end{aligned}$$

The approximate absorption coefficient (2.29) has a linear relationship with frequency Δ in the region of the energy gap. This behavior is similar to the one-photon forbidden transitions.

The approximate result (2.29) may be derived by a simple argument which avoids our tedious derivation. When we evaluate the sum over intermediate states in (2.6), a simple approximation is to neglect the exciton energy in the energy denominator. This is equivalent to approximating the Coulomb Green's function by

$$G(r,0) \simeq (\kappa^2/E_B) \delta(r),$$

and (2.6) becomes

$$I_\delta(\alpha,\beta) = -i(\hbar\kappa_\alpha^2/E_B) [\hat{\epsilon}_\beta \cdot \nabla \psi_\delta(r)]_{r=0}. \quad (2.30)$$

When the result (2.30) is used to calculate the attenuation constant, then one immediately gets (2.29). The approximate result for the matrix element I_δ depends upon the derivative of the hydrogenic wave function at $r=0$. This feature makes the two-quantum allowed transition resemble the one-quantum forbidden transition, since the latter have a similar dependence. It is interesting that, with the Wannier model, the result (2.30) is exact for one-photon transition to p states, but is only approximate for two-photon transitions. The approximation (2.30) was used in the calculations of Ref. 11.

D. Numerical Results

Numerical calculations were made in order to compare the exact and approximate solutions. The two polarizations $\hat{\epsilon}_1$ and $\hat{\epsilon}_2$ were assumed to be parallel. The first set of parameters were characteristic of an alkali halide; $E_G=7.0$ eV, $E_B=0.5$ eV, and $\hbar\omega_1=1.5$ eV. For these parameters, $\kappa_1=0.30$, and $0.50 < \kappa_2 < 1.0$, for the range of $\hbar\omega_2$ which is shown. For these large values of κ , the approximate formulas do not predict the same shape of attenuation curve as the exact formulas. This conclusion agrees with the original hypothesis that the approximate results were only valid at small κ .

The same type of calculation is done in Fig. 1(b) for parameters which are typical for a semiconductor, with $E_G=2.5$ eV, $E_B=0.03$ eV, and the laser frequency $\hbar\omega_1=1.0$ eV is in the neodymium range. These numbers give $\kappa_1=0.14$, while κ_2 varies between 0.17 and 0.18 for the range of $\hbar\omega_2$ which is shown in Fig. 1(a). In these figures we plot the dimensionless function $\alpha^p/(P_1 C_A)$, and the approximate result (2.29) is dotted while the solid line is the exact attenuation coefficient (2.19) and (2.26). We have started these functions in the vicinity of the $n=2$ line, although (2.19) and (2.29) actually vanish linearly at the $n=1$ line. In the second case Fig. 1(b) where the κ 's are small, the approximate formulas work quite well.

The approximate formulas do predict the correct magnitude of the absorption coefficient even for large κ , and hence are useful for order-of-magnitude estimates of absorption strengths. For this purpose we note that the constant C_A is directly proportional to the one-photon absorption constant.

In Fig. 1(a), the exact absorption coefficient is diverging at $\hbar\omega_1 + \hbar\omega_2 = 8.0$ eV because this coincides with the real absorption line at $\hbar\omega_2 = E_G - E_B = 6.5$ eV. The approximate formula does not diverge here because κ_2 does not become large until $\hbar\omega_2 = E_G$. We tried improving the approximate equation by replacing κ_α^2 by $(\kappa_\alpha^{-2} - 1)^{-1}$ in (2.29). Although this makes the approximate equation diverge at the right frequency, it still does not resemble the exact result, and this modification was abandoned.

III. FORBIDDEN DIPOLE TRANSITION

We now consider the case where the conduction-band to valence-band dipole matrix element is forbidden at $k=0$. Although the transition probability and matrix element are still given by (2.1) and (2.2), the spectral dependence of the attenuation coefficient is quite different than when the transitions are allowed.

For forbidden dipole transitions, the matrix element between the initial and intermediate state is^{18,19}

$$\begin{aligned} \langle l | \hat{\epsilon}_\alpha \cdot \mathbf{p} | i \rangle &= i\hbar\sqrt{V} [\hat{\epsilon}_\alpha \cdot \mathbf{M} \cdot \nabla \psi_\lambda(r)]_{r=0} \\ &= i\hbar\sqrt{V} \hat{\epsilon}_{\alpha\mu} M_{\mu\nu} (\partial/\partial x_\nu) \psi_\lambda(r)_{r=0}. \end{aligned} \quad (3.1)$$

¹⁸ R. J. Elliott and R. Loudon, J. Phys. Chem. Solids 8, 382 (1959).

¹⁹ R. J. Elliott, Phys. Rev. 124, 340 (1961).

The matrix $M_{\mu\nu}$ was introduced by Elliott and Loudon¹⁸ in their discussion of the forbidden one-photon transition. They showed from $\mathbf{k}\cdot\mathbf{p}$ theory that $M_{\mu\nu}$ has the form

$$M_{\mu\nu}(l,i) = \frac{1}{m} \sum_j \left\{ \frac{\langle l | \hat{p}_\mu | j \rangle \langle j | \hat{p}_\nu | i \rangle}{E_l - E_j} + \frac{\langle l | \hat{p}_\nu | j \rangle \langle j | \hat{p}_\mu | i \rangle}{E_i - E_j} \right\}. \quad (3.2)$$

This is the definition of the inverse effective mass tensor^{20,21} when $l=i$, but in the optical problem we explicitly want the case $l \neq i$.

The other matrix element is still given by (2.5), so we now need to evaluate the sum over intermediate exciton states for the following integral.

$$I_\delta(\alpha,\beta) = -i\hbar\epsilon_{\alpha\mu}M_{\mu\nu} \int d^3r \psi_\delta^*(r) \hat{\epsilon}_\beta \cdot \mathbf{p} \times \sum_\lambda \frac{\psi_\lambda(r)}{E_\lambda + E_G - \hbar\omega_\alpha} \frac{\partial}{\partial x_\nu'} \psi_\lambda^*(r')_{r'=0}. \quad (3.3)$$

If we include spin-orbit effects in the Hamiltonian, then P_ν should be replaced by²²

$$\mathbf{P} + \frac{\hbar}{4mC^2} \boldsymbol{\sigma} \times \boldsymbol{\Delta} V.$$

This refinement is apparently important in zinc blende, where matrix elements exist for the spin-orbit term which vanish for the \hat{p} term.²² This will make $M_{\mu\nu}$ finite, and hence allow transitions, where otherwise they would not be permitted. This apparently is important in CuCl, and this point is discussed in Sec. IV. In crystals which lack an inversion center, these "forbidden" transitions are allowed along with the \hat{p} -state transitions of Sec. II. Actually, the exciton s - and d -state transitions are allowed whenever the matrix $M_{\mu\nu}$ is finite.

The sum over intermediate states in (3.3) can be expressed as a gradient of the Coulomb Green's function

$$\begin{aligned} \lim_{r' \rightarrow 0} \frac{\partial}{\partial x_\nu'} G(r, r') &= \lim_{r' \rightarrow 0} \sum_\lambda \frac{\psi_\lambda(r)}{E_\lambda + E_G - \hbar\omega_\alpha} \frac{\partial}{\partial x_\nu'} \psi_\lambda(r') \\ &= \frac{-x_\nu \Gamma(2-\kappa) \bar{\mu}}{2\pi\kappa a r^2 \hbar^2} W_{\kappa, 3/2} \left(\frac{2r}{a\kappa} \right), \end{aligned} \quad (3.4)$$

where κ is defined in (2.8). Thus in (3.3) we are basically

²⁰ J. M. Luttinger and W. Kohn, Phys. Rev. **97**, 869 (1955).

²¹ E. I. Blount, in *Solid State Physics*, edited by F. Seitz and D. Turnbull (Academic Press Inc., New York, 1962), Vol. 5, p. 305.

²² G. Dresselhaus, Phys. Rev. **100**, 580 (1955); R. H. Parmenter, *ibid.* **100**, 573 (1955); V. Heine, *Group Theory in Quantum Mechanics* (Pergamon Press, Inc., New York, 1960).

trying to evaluate

$$I_\delta(\alpha,\beta) = \hbar^2 \epsilon_{\alpha\mu} M_{\mu\nu} \epsilon_{\beta\lambda} \int d^3r \times \psi_\delta^*(r) \frac{\partial}{\partial x_\lambda} \frac{x_\nu \Gamma(2-\kappa) \bar{\mu} W_{\kappa, 3/2}(2r/a\kappa)}{2\pi\kappa a r^2 \hbar^2}. \quad (3.5)$$

At this point the calculation divides itself into two parts. The first is the actual evaluation of the integral in (3.5). Secondly, one must derive the general form of $M_{\mu\nu}$ from group theory and discuss the polarization dependence of the absorption coefficient. The complexity of the calculation is summarized by noting that we can have $\lambda=\nu$ or $\lambda \neq \nu$ in (3.5), the final states are either s or d exciton states, and $M_{\mu\nu}$ has four different possible forms in cubic materials. In Secs. III A through III D we evaluate the integral in (3.5), and in Sec. III F we give the final results with the correct polarization dependences.

A. d -Exciton Bound States

Let us first consider the case where $\nu \neq \lambda$ in (3.5). Then the final-state wave function ψ_δ must have the symmetry $x_\nu x_\lambda$ in order that the integral not vanish. This requires ψ_δ to be an exciton d state. We assume the d states are fivefold degenerate. Instead of the usual spherical harmonics $Y_{l,m}$, it is more convenient to introduce the five orthonormal harmonics

$$\begin{aligned} Y_{2,0} &= \left(\frac{5}{16\pi} \right)^{1/2} \frac{2z^2 - x^2 - y^2}{r^2}, & Y_{2,xy} &= \left(\frac{15}{4\pi} \right)^{1/2} \frac{xy}{r^2}, \\ Y_{2,a} &= \left(\frac{15}{16\pi} \right)^{1/2} \frac{x^2 - y^2}{r^2}, & Y_{2,xx} &= \left(\frac{15}{4\pi} \right)^{1/2} \frac{zx}{r^2}, \\ Y_{2,yz} &= \left(\frac{15}{4\pi} \right)^{1/2} \frac{yz}{r^2}. \end{aligned} \quad (3.6)$$

When $\nu \neq \lambda$ in (3.5), the exciton final d state will have the symmetry of either $Y_{2,xy}$, $Y_{2,yz}$, or $Y_{2,xx}$. All of these states will have the same absorption coefficients. For example, the integration over angles in (3.5) gives

$$\begin{aligned} \int d\Omega Y_{2,xy} \frac{\partial}{\partial x} \left\{ \frac{y}{r^2} W_{\kappa, 3/2} \left(\frac{2r}{a\kappa} \right) \right\} \\ = \left(\frac{4\pi}{15} \right)^{1/2} \frac{\partial}{\partial r} \left[r^{-2} W_{\kappa, 3/2} \left(\frac{2r}{a\kappa} \right) \right], \end{aligned} \quad (3.7)$$

which is independent of the choice xy . The derivative in (3.7) is easily performed by letting the Whittaker's function be¹⁶

$$W_{\kappa, 3/2}(z) = \frac{z^2 e^{-z/2}}{\Gamma(2-\kappa)} \int_0^\infty dt e^{-zt} t^{1-\kappa} (1+t)^{1+\kappa}. \quad (3.8)$$

Furthermore, the r integral can be done using (2.12)

and we get for (3.5)

$$I_{n,l=2}(\alpha,\beta) = \frac{\epsilon_{\alpha\mu} M_{\mu\nu} \epsilon_{\beta\lambda} \bar{\mu}}{(15\pi a^3)^{1/2}} \times \left[\frac{(1-1/n^2)(1-4/n^2)}{n^3} \right]^{1/2} J_{d,n}(\kappa), \quad (3.9)$$

$$J_{d,n}(\kappa) = \kappa^2 \int_0^\infty dt (t+\frac{1}{2}) t^{1-\kappa} (1+t)^{1+\kappa} \frac{(t+\frac{1}{2}-\kappa/2n)^{n-3}}{(t+\frac{1}{2}+\kappa/2n)^{n+3}}. \quad (3.10)$$

The integral (3.10) is very similar to the p -wave result (2.14). The d -wave term (3.10) may also be expressed as a series expansion

$$J_{d,n}(\kappa) = \frac{\kappa^2 \Gamma(2-\kappa)}{t_0^{3+\kappa}} \sum_{l=0}^{n-3} (3-n)_l \left(\frac{\kappa}{nt_0} \right)^l (l+1) \times \left[\frac{{}_2F_1(2-\kappa, -1-\kappa; l+4-\kappa, 1-t_0)}{\Gamma(l+4-\kappa)} \right. \\ \left. - \frac{(l+2)\kappa {}_2F_1(2-\kappa, -1-\kappa; l+5-\kappa, 1-t_0)}{2nt_0 \Gamma(l+5-\kappa)} \right]. \quad (3.11)$$

The same comments which applied to (2.15) also apply to (3.11): This expression is useful for evaluating $J_{d,n}$ for all n where $\kappa/n < 1$. It is particularly useful for evaluating the transition probability to the first d state at $n=3$.

Since the matrix element can be evaluated using (3.11), the absorption coefficient can now be given. There are two matrix elements $J_{d,n}(\kappa_1)$ and $J_{d,n}(\kappa_2)$ since the photons can be absorbed in either order. This is evident in (2.2). These two terms do not necessarily add coherently. Depending upon the form of $M_{\mu\nu}$, these two terms may be combined with different relative phases. We anticipate our later results by stating that only two cases are necessary—the case where they add and the case where they subtract. We define these as the symmetric α_d^S and antisymmetric α_d^A absorption coefficient.

$$\alpha_d^S = P_1 C_F \frac{3}{80} (1-n^{-2})(1-4n^{-2}) \left(\frac{2S_n E_B}{n^3} \right) \times \left(\frac{E_B^3}{\hbar^3 \omega_1^2 \omega_2} \right) |J_{d,n}(\kappa_1) + J_{d,n}(\kappa_2)|^2, \quad (3.12a)$$

$$\alpha_d^A = P_1 C_F \frac{3}{80} (1-n^{-2})(1-4n^{-2}) \left(\frac{2S_n E_B}{n^3} \right) \times \left(\frac{E_B^3}{\hbar^3 \omega_1^2 \omega_2} \right) |J_{d,n}(\kappa_1) - J_{d,n}(\kappa_2)|^2, \quad (3.12b)$$

$$C_F = \frac{2^7 \pi^2 \hbar^5 (e^2)^2 |M_{\mu\nu}|^2}{3^2 n_2 (\hbar c) E_B^4 a^3 m^2}. \quad (3.13)$$

The only difference between α_d^S and α_d^A is the plus or minus in the last bracket. The particular choice for C_F , which gives the 3/80 factor in (3.12), is convenient for the s -state absorption coefficient which is derived below. The polarization dependence has been removed from (3.13) and we just use $|M_{\mu\nu}|^2$, when $M_{\mu\nu}$ is one component of the tensor. This usage will be clarified in Sec. III F. When the bound states become densely packed, then $2S_n E_B/n^3 \rightarrow 1$, as was done also for p states.

B. d -Exciton Continuum States

When the sum of the two photon frequencies $\hbar\omega_1 + \hbar\omega_2$ exceeds the energy gap E_G , and when $\nu \neq \lambda$ in (3.5), the final state of the exciton will be in the continuum with d symmetry. Hence we want the $l=2$ state in (2.20). If we remember that $\cos\omega$ is the angle between \mathbf{k} and \mathbf{r} , then

$$\int d\Omega P_2(\cos\omega) \frac{\partial}{\partial x} \left[\frac{y}{r^2} W_{\kappa,3/2} \left(\frac{2r}{a\kappa} \right) \right] \\ = \left(\frac{4\pi}{5} \right)^{1/2} \frac{k_x k_y}{k^2} r \frac{\partial}{\partial r} \left[\frac{1}{r^2} W_{\kappa,3/2} \left(\frac{2r}{a\kappa} \right) \right]. \quad (3.14)$$

Here we have chosen $x_\lambda = x$, $x_\nu = y$, but the results will be independent of this choice. Now the sum over intermediate states in (3.5) becomes

$$I_{k,l=2}(\alpha,\beta) = \frac{\bar{\mu} a^2}{\sqrt{V}} k_\nu k_\lambda \epsilon_{\alpha\mu} M_{\mu\nu} \epsilon_{\beta\lambda} \times e^{\eta\pi/2} |\Gamma(3-i\eta)| J_{d,k}(\kappa), \quad (3.15)$$

$$J_{d,k}(\kappa) = \kappa^2 \int_0^\infty dt t^{1-\kappa} (1+t)^{1+\kappa} (t+\frac{1}{2}) \times \left(t+\frac{1}{2} - \frac{i\kappa}{2\eta} \right)^{-(3+i\eta)} \\ \times \left(t+\frac{1}{2} + \frac{i\kappa}{2\eta} \right)^{-(3-i\eta)}, \quad (3.16)$$

$$= 4\kappa^2 \int_0^1 dS S \frac{(1-S)^{1-\kappa} (1+S)^{1+\kappa}}{[1+(S\kappa/\eta)^2]^3} \times \exp\left(-2\eta \tan^{-1} \frac{S\kappa}{\eta}\right). \quad (3.17)$$

The integral (3.17) was derived in the same way as the p -state result (2.24). This was the form used in the numerical calculations.

Since the sum over intermediate states has been evaluated in (3.15), the attenuation coefficient can now be evaluated. When we sum over the final states, this leads to an angular average $\langle k_x^2 k_y^2 \rangle = k^4/15$. Again we need to define a symmetric and antisymmetric absorp-

tion coefficient.

$$\alpha_d^{S,A} = P_1 C_F \frac{3(1+\eta^{-2})(1+4\eta^{-2})}{80} \frac{E_B^3}{1-e^{-2\pi\eta}} \frac{E_B^3}{\hbar^3 \omega_1^2 \omega_2} \times |J_{d,k}(\kappa_1) \pm J_{d,k}(\kappa_2)|^2. \quad (3.18)$$

The coefficient C_F is given in (3.13). The d -state absorption coefficient is continuous at the energy gap, i.e., the result (3.18) for $\eta \rightarrow \infty$ joins smoothly to (3.12) as $n \rightarrow \infty$ and $S_n = n^3/2E_B$. Using our definition (2.26') of $\eta^{-2} \equiv \Delta = (\hbar\omega_1 + \hbar\omega_2 - E_G)/E_B$, we see from (3.18) that the attenuation coefficient rises parabolically with Δ when Δ is small.

Approximate solutions for the d -state absorption coefficient can be obtained when κ is small—as was done for p states. When κ is small, we get [from (3.17) and (3.11)]

$$\begin{aligned} J_{d,n}(\kappa) &= \kappa^2 [1 + O(\kappa)], \\ J_{d,k}(\kappa) &= \kappa^2 [1 + O(\kappa)]. \end{aligned} \quad (3.19)$$

The approximation (3.19) may be used in evaluating (3.12) and (3.18). As in the p -state case, the approximate formulas (3.19) are very good when κ is small ($\kappa < 0.2$). However, even when κ is large (~ 0.5), the results (3.19) give the magnitude of J to within 50%.

The approximate results (3.19) can be derived in a simple way. As in the derivation of (2.30), if we ignore the exciton energy in the sum over intermediate states, then (3.5) is given by

$$I_{k,l=2}(\alpha,\beta) = \frac{\hbar^2 \kappa^2}{E_B} \epsilon_{\alpha\mu} M_{\mu\nu} \epsilon_{\beta\lambda} \left(\frac{\partial}{\partial x_\nu} \frac{\partial}{\partial x_\lambda} \psi_\delta(r) \right)_{r=0}. \quad (3.20)$$

When the absorption coefficient is evaluated from (3.20), one immediately obtains the results (3.12) and (3.18) but with $J_d = \kappa^2$.

C. s -Exciton States

We now consider the evaluation of (3.5) for the case that $\nu = \lambda$. The derivative gives

$$\frac{\partial}{\partial x_\nu} \left[\frac{x_\nu}{r^2} W_{\kappa,3/2} \left(\frac{2r}{a\kappa} \right) \right] = \frac{W_{\kappa,3/2}}{r^2} + \frac{x_\nu^2}{r} \frac{\partial}{\partial r} \left(\frac{W_{\kappa,3/2}}{r^2} \right). \quad (3.21)$$

The first term in (3.21) is spherically symmetric, and this requires that the exciton state be an s state. Furthermore, the x_ν^2 term will be a combination of the spherical harmonics $Y_{l=0}$ for s waves, and $Y_{2,0}$ and $Y_{2,\alpha}$ in (3.6). Therefore the terms in (3.21) creates both s and d states. Since one evaluates the absorption coefficient separately for each final states, we will just evaluate the s -wave part here. The d -wave contribution from (3.21) will just be proportional to α_d which was derived in the preceding sections. The proper proportionality between s and d which results from (3.21) is simple,

and the derivation of this result will be given below in Sec. III F and Appendix II.

The angular average of $\langle x_\nu^2 \rangle$ is $1/3r^2$, so that (3.21) may be rewritten for s states as

$$\frac{1}{3r^2} \frac{\partial}{\partial r} \left[r W_{\kappa,3/2} \left(\frac{2r}{a\kappa} \right) \right].$$

The evaluation of the integral in (3.5) proceeds as it did for p and d states. The result is

$$I_{n,l=0}(\alpha,\beta) = \frac{(\hat{\epsilon}_\alpha \cdot \mathbf{M} \cdot \hat{\epsilon}_\beta) 4\bar{\mu}}{3\sqrt{\pi} a^{3/2} \eta^{3/2}} J_{s,n}(\kappa_\alpha), \quad (3.22)$$

where

$$\begin{aligned} J_{s,n}(\kappa_\alpha) &= \frac{\kappa}{8n} \int_0^\infty dt t^{1-\kappa} (1+t)^{1+\kappa} \\ &\times \left[(n+1)(n+2) \frac{(t+\frac{1}{2}-\kappa/2n)^{n-1}}{(t+\frac{1}{2}+\kappa/2n)^{n+3}} \right. \\ &\left. - (n-1)(n-2) \frac{(t+\frac{1}{2}-\kappa/2n)^{n-3}}{(t+\frac{1}{2}+\kappa/2n)^{n+1}} \right]. \end{aligned} \quad (3.23)$$

This may also be expressed as a series

$$\begin{aligned} J_{s,n}(\kappa) &= \frac{\kappa}{8(2-\kappa)n!0^{2+\kappa}} \sum_{l=0}^{n-1} \left(\frac{\kappa}{n!0} \right)^l \frac{(1-n)_l (2n-l)(l+3)}{(3-\kappa)_l} \\ &\times {}_2F_1(2-\kappa, -1-\kappa, l+3-\kappa, 1-l_0). \end{aligned} \quad (3.24)$$

Similarly, the symmetric and antisymmetric absorption coefficients to an exciton bound s state are

$$\begin{aligned} \alpha_s^{S,A} &= P_1 C_F \left(\frac{S_n 2E_B}{n^3} \right) \frac{E_B^3}{\hbar^3 \omega_1^2 \omega_2} \\ &\times |J_{s,n}(\kappa_1) \pm J_{s,n}(\kappa_2)|^2. \end{aligned} \quad (3.25)$$

The constant C_F is the same as C_F in (3.13).

The absorption coefficient for exciton s states in the continuum can be derived by the methods which have been employed above for p and d states.

$$\alpha_s^{S,A} = P_1 C_F \frac{E_B^3}{\hbar^3 \omega_1^2 \omega_2} \frac{|J_{s,k}(\kappa_1) \pm J_{s,k}(\kappa_2)|^2}{1-e^{-2\pi\eta}}, \quad (3.26)$$

where

$$\begin{aligned} J_{s,k}(\kappa) &= \frac{\kappa}{2\eta} \int_0^1 ds \frac{(1+s)^{1+\kappa} (1-s)^{1-\kappa}}{[1+(s\kappa/\eta)^2]^3} \\ &\times \left[3\eta \left(1 - \frac{s^2 \kappa^2}{\eta^2} \right) + \frac{2\kappa s}{\eta} (2-\eta^2) \right] \\ &\times \exp \left(-2\eta \tan^{-1} \frac{s\kappa}{\eta} \right). \end{aligned} \quad (3.27)$$

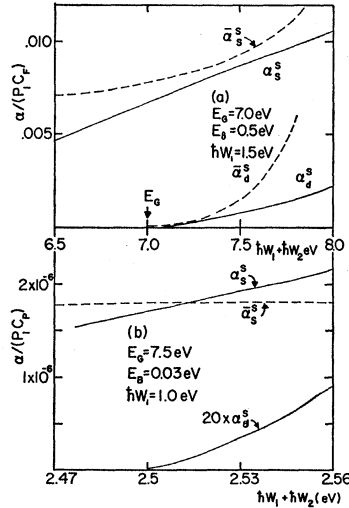


FIG. 2. The two photon-absorption coefficient for excitons s and d states. The approximate formulas are dotted. Just the symmetric coefficients are shown. The antisymmetric coefficients (α^A) have a similar spectral dependence but are smaller in magnitude. In (a), the parameters are characteristic of an alkali halide. In (b), the parameters describe a semiconductor with a small exciton energy. The d -state coefficient α_d^S has been magnified 20 times, and the approximate $\bar{\alpha}_d^S$ is not shown, since it coincides with α_d^S .

The absorption coefficient above the energy gap (3.21) is continuous with that below the gap; the latter given by (3.25) with $S_n = n^3/2E_B$ for large n values.

D. Approximations to s -State Absorption

In the limit of small κ , we can obtain approximations to $J_{s,n}(\kappa)$ and $J_{s,k}(\kappa)$ by expanding them in a power series in κ . The leading terms are

$$\begin{aligned} J_{s,n}(\kappa) &= \kappa[1 + O(\kappa)], \\ J_{s,k}(\kappa) &= \kappa[1 + O(\kappa)]. \end{aligned} \quad (3.28)$$

The leading terms are proportional to κ . This is quite different than the κ^2 dependence for p and d states which is found in (2.28) and (3.19). This difference is quite important in affecting the shape and magnitude of the s -state absorption curve.

Some insight into why the s state is different from the p and d is obtained by trying to derive an approximate formula for s -state absorption. For p and d states, we could derive the correct approximate result by just ignoring the exciton energy in the sum over intermediate states (2.6) or (3.3). This method does not work for s states. Such an approximation gives (3.20) with $x_\nu = x_\lambda$, e.g., (3.20) becomes (for $x_\nu = x_\lambda = x$)

$$I_{s,l=0} = \frac{\kappa^2 \hbar^2}{E_B} (\hat{\epsilon}_\alpha \cdot \mathbf{M} \cdot \hat{\epsilon}_\beta) \left[\frac{\partial^2}{\partial x^2} \psi_{n,l=0}(r) \right]_{r \rightarrow 0}. \quad (3.29)$$

The quantity in brackets diverges as $r \rightarrow 0$ for hydrogenic wave functions. If we take (3.22) with $J_{s,n} \sim \kappa$, and compare this to (3.29), we see that one should make the

replacement

$$\left[\frac{\partial^2}{\partial x^2} \psi_{n,l=0} \right]_{r=0} \rightarrow \frac{2\psi_{n,0}(0)}{3a^2\kappa}. \quad (3.30)$$

We should emphasize that the divergence in (3.29) exists only in the attempt in (3.20) to find an approximate formula. The rigorous solution presented in Eqs. (3.21)–(3.27) does not have any problems with divergences. Furthermore, these divergences are avoided by making (3.22) and (3.28) the basis for our approximate solutions.

E. Numerical Results for s and d States

Some numerical calculations were performed in order to determine the frequency dependence of the various absorption coefficients. For this purpose it is convenient to neglect the polarization dependence of the matrix elements, and just to evaluate the magnitude of the absorption coefficient. Results are just given for the symmetric coefficient α_s^S and α_d^S . The antisymmetric coefficients α_s^A and α_d^A have a similar frequency dependence to their α^S counterpart, but are smaller in magnitude. Basically we are plotting

$$\begin{aligned} \alpha_d^S / (P_1 C_F) &= \frac{3}{80} (1 + \Delta)(1 + 4\Delta) \frac{E_B^3}{\hbar^3 \omega_1^2 \omega_2} |J_d(\kappa_1) + J_d(\kappa_2)|^2, \\ \alpha_s^S / (P_1 C_F) &= \frac{E_B^3}{\hbar^3 \omega_1^2 \omega_2} |J_s(\kappa_1) + J_s(\kappa_2)|^2, \end{aligned}$$

where $\Delta = (\hbar\omega_1 + \hbar\omega_2 - E_G)/E_B$, and $T(\Delta)$ is defined in (2.29).

The notation J_d means $J_{d,n}$ for bound states and $J_{d,k}$ for continuum states. These are calculated from (3.11) and (3.17) for the exact absorption coefficient, while $J_d \sim \kappa^2$ was used in the approximate expressions. Similarly, J_s means either (3.23) or (3.27), with $J_s \sim \kappa$ used as the approximate formula.

These numerical results are shown in Fig. 2 for the same two sets of parameters which were employed in Fig. 1. Approximate expressions are denoted $\bar{\alpha}$. The d -state coefficient α_d is given reasonably well by the approximate expression. The quadratic rise of α_d with $\hbar\omega_2 + \hbar\omega_1$ is caused by the $(1 + \Delta)(1 + 4\Delta)$ factor. The shape of the s -state coefficient is much different than its approximate form. This is because $J_{s,n}$ and $J_{s,k}$ have a large n and k dependence even when κ is small. The approximation $J_s \sim \kappa$ does give the correct magnitude of the absorption coefficient. However, it is obvious that one must use the exact definitions for J_s for any detailed comparison of experiment and theory.

The magnitudes of α_s and α_d can be compared directly since the same coefficient C_F enters both expressions. At the energy gap ($\Delta = 0$), their ratio is $\alpha_d/\alpha_s \sim 3\kappa^2/80$. Since $\kappa < 1$, α_d is much smaller than α_s . However, as Δ

increases when one goes above the energy gap, the α_d value increases much faster. Thus, in Fig. 2(a) where $\kappa > 0.5$, the α_d absorption can become comparable to α_s . However, in the case of Fig. 2(b), where $\kappa < 0.2$, the d -state absorption is always negligible. In order to compare α_p with α_s or α_d , one must explicitly know the values of $M_{\mu\nu}$ which as yet are not known.

F. Polarization Dependences

It was already noted in Sec. III A that the p -state absorption in cubic materials has an angular dependence upon the polarization of the incident photons. The s - and d -state absorptions also have a strong polarization dependence. Inoue and Toyozawa¹⁰ calculated those dependencies for s -state absorption. In the case of cubic symmetry (O_h), we have extended their results to include the d states as well.

We will briefly summarize their s -state results. The ground state of system, before the photons enter, is obviously A_{1g} . Absorption of two photons (T_{1u}) takes the electronic system into states with the symmetry $T_{1u} \times T_{1u} = A_{1g} + E_g + T_{1g} + T_{2g}$. These four final states have different polarization dependences, which allows them to be easily distinguished experimentally. If we introduce the direction cosines $\hat{\epsilon}_1 = (l_1, m_1, n_1)$, $\hat{\epsilon}_2 = (l_2, m_2, n_2)$, then they showed that

$$(\hat{\epsilon}_1 \cdot \mathbf{M} \cdot \hat{\epsilon}_2)^2 = |M(f_j)|^2 f_j(\hat{\epsilon}_1, \hat{\epsilon}_2),$$

where f_j is one of the four functions

$$A_{1g} = (\hat{\epsilon}_1 \cdot \hat{\epsilon}_2)^2 = (l_1 l_2 + m_1 m_2 + n_1 n_2)^2, \quad (3.31)$$

$$E_g = l_1^2 l_2^2 + m_1^2 m_2^2 + n_1^2 n_2^2 - (l_1 l_2 m_1 m_2 + l_1 l_2 m_1 n_2 + n_1 n_2 m_1 m_2), \quad (3.32)$$

$$T_{1g} = (\hat{\epsilon}_1 \times \hat{\epsilon}_2)^2 = 1 - (\hat{\epsilon}_1 \cdot \hat{\epsilon}_2)^2, \quad (3.33)$$

$$T_{2g} = 1 - (l_1^2 l_2^2 + m_1^2 m_2^2 + n_1^2 n_2^2) + 2(l_1 l_2 m_1 m_2 + l_1 l_2 n_1 n_2 + n_1 n_2 m_1 m_2). \quad (3.34)$$

These results can be easily deduced from symmetry. For example, $M(A_{1g})_{\mu\nu}$ is a symmetric second-rank tensor, which, because of cubic symmetry, must have the form $M(A_{1g})_{\delta\mu\nu}$; this leads directly to (3.31). In the T_{2g} transition, the final T_{2g} state is threefold degenerate and we label these states (x, y, z) . The appropriate tensor is symmetric:

$$M_{\mu\nu}^{(j)}(T_{2g}) = M_{\nu\mu}^{(j)}(T_{2g}),$$

where $(j) = (x, y, z)$ for the three final T_{2g} states. This has nonzero components

$$M_{\mu\nu}^{(j)}(T_{2g}) = M_{xy}^{(x)} = M_{yz}^{(x)} = M_{zx}^{(y)}. \quad (3.35)$$

This leads directly to the result (3.34). Similarly, the T_{1g} tensor has the same form as (3.35) but it is antisymmetric. Proceeding in this way, one can show that the results of Inoue and Toyozawa follow directly from the properties of the $M_{\mu\nu}$ matrix introduced by Elliott and Loudon.¹⁸

It is worth noting that there are only two independent angular functions. One can denote them as

$$D_1 = l_1^2 l_2^2 + m_1^2 m_2^2 + n_1^2 n_2^2,$$

$$D_2 = l_1 l_2 m_1 m_2 + l_1 l_2 n_1 n_2 + m_1 m_2 n_1 n_2.$$

All of the functions in (3.31)–(3.34) can be expressed as linear combinations of 1, D_1 , and D_2 . That is, only two of the functions A_{1g} , E_g , T_{1g} , and T_{2g} are really independent. If we choose A_{1g} and E_g as the independent pair, then

$$T_{1g} = 1 - A_{1g},$$

$$T_{2g} = 1 + A_{1g}/3 - 4E_g/3.$$

This remark is not very important for s states. But for d states, when the answer comes out a linear combination of 1, D_1 , and D_2 , it can be expressed as a large number of different combinations of A_{1g} , E_g , T_{1g} , and T_{2g} .

As we noted above, absorption to the s and d states occurs simultaneously, at least above the $n=3$ line where the d -state absorption begins. The polarization dependence for the combined absorption is

$$\begin{aligned} A_{1g}: \quad \alpha &= \alpha_d^s + (\alpha_s^s + \frac{1}{3}\alpha_d^s)A_{1g}, \\ E_g: \quad \alpha &= (\alpha_s^s + \frac{1}{3}\alpha_d^s)E_g + \frac{3}{4}\alpha_d^s T_{1g} \\ &\quad + \frac{1}{4}\alpha_d^s(1 + 3A_{1g}), \\ T_{1g}: \quad \alpha &= (\alpha_s^s + \frac{5}{6}\alpha_d^s)T_{1g} + \alpha_d^s(3 + A_{1g}), \\ T_{2g}: \quad \alpha &= (\alpha_s^s + \frac{5}{6}\alpha_d^s)T_{2g} + \frac{3}{2}\alpha_d^s T_{1g} \\ &\quad + \frac{3}{2}\alpha_d^s(E_g + A_{1g}). \end{aligned} \quad (3.36)$$

The angular functions A_{1g} , E_g , T_{1g} and T_{2g} are given in (3.31)–(3.34). The $\alpha_s^{s,A}$ and $\alpha_d^{s,A}$ are defined in (3.12), (3.18), (3.25), and (3.26). In the definition of C_F in (3.13), $|M_{\mu\nu}|^2$ means the nonzero tensor component, such as (3.35). An example of how to derive these results is given in Appendix II.

Our results for s states verify the results of Inoue and Toyozawa.¹⁰ An additional feature of our results is that the T_{1g} angular functions are always associated with antisymmetric absorption coefficients α_s^A , α_p^A , and α_d^A . Since the antisymmetric functions are generally smaller than the symmetric ones, the T_{1g} symmetry may be harder to see experimentally. In general the angular dependence of d -state coefficients is quite complicated.

IV. COMPARISON WITH EXPERIMENTS

Alkali halides: The original two-photon experiments of Hopfield *et al.*¹ were on KI and CsI. Many other alkali halides were measured by Frohlich and Stagginnus.² Here the direct transition is allowed, so the absorption creates final p -state excitons. After the initial onset near the $n=2$ line, the low-temperature absorption coefficient appears to rise linearly with frequency. This agrees with the present theory. Indeed, our approximate solution for p states, which had been

derived earlier,¹¹ was used by Hopfield and Worlock¹ in the analysis of their results. No discrete bound states have been observed. This is because the first p state at $n=2$ is too close to the other exciton lines ($n=3,4$, etc.), and the width is too large.

We have previously reported¹² a comparison of our calculated results with the experiments of Frohlich and Stagginnus on RbI.² There were three parts to this comparison. First, the magnitude of the two-photon absorption was calculated using (2.18) and (2.26). The coefficient C_A in (2.18b) was found by obtaining $\langle c|p_x|v\rangle$ from the one-photon absorption. The other parameters $E_B=0.5$ eV, $E_G=6.25$ eV, $\hbar\omega_1=1.785$ eV, and laser power were obtained from Ref. 2. The calculated magnitude was exactly that which was observed. This agreement is pleasant but partly fortuitous, since some of the parameters are not known precisely, especially the one-photon absorption coefficient and also the refractive indices near the band gap. Second, the spectral dependence of the absorption coefficient was evaluated and this also agreed with the experimental observation. Third, the observed polarization dependence was precisely that predicted by (2.17). At 6.8 eV in Rb, Frohlich and Stagginnus showed that the absorption coefficient changed as the angle θ changed. The ratio between the minimum and maximum absorption at this energy is

$$R = \frac{\alpha(\theta = \frac{1}{2}\pi)}{\alpha(\theta = 0)} = \frac{J_p(\kappa_1)^2 + J_p(\kappa_2)^2}{|J_p(\kappa_1) + J_p(\kappa_2)|^2}. \quad (4.1)$$

From their data we deduce that this ratio is about 0.62, while we calculated the value 0.69. This ratio is limited to values between one-half and one.

CuCl: Frohlich and co-workers⁵ have recently observed some discrete excitons in CuCl using two-photon spectroscopy. This is a zinc-blende structure, so the group theoretical selection rules are quite different than in the alkali halides.²² These sharp lines were identified as exciton s states by their energy position, and also because they had the polarization dependence (3.34) associated with a T_2 state (Γ_5 in their notation²³). They also commented that the Γ_5 type polarization dependence was not observed for transitions to the exciton continuum—here they described the behavior as “rather complex.”

Since the dipole transition is allowed between the conduction (Γ_6) and valence bands (Γ_7 and Γ_8), one would expect from our result that the main absorption to the continuum is caused by exciton p states. The p -state absorption would also be dependent on the photon polarization vectors. Perhaps the “rather

complex” polarization dependence observed in the exciton continuum is caused by a combination of α_s , α_p , and α_d absorption. No bound excitons in p states are observed, nor are any $n=2$, s states. The two s states observed in the spectra are the $n=1$ states from the two valence bands. This follows from the interpretation of the one-photon spectra given by Cardona.²⁴

The oscillator strength of the observed discrete exciton state appears small compared with the oscillator strength in the continuum. This suggests that s -state absorption is weaker than the transition which is causing most of the continuum absorption, which is presumably a p state. The magnitude of the “forbidden” transition to s states depends upon the size of $M_{\mu\nu}$ in (3.2). If we ignore spin-orbit effects, the term $M_{\mu\nu}$ vanishes in zinc-blende structures.²² Including spin-orbit effects causes $M_{\mu\nu}$ to be finite. There is a close relationship here to the linear wave vector term, which also exist because of the spin-orbit interaction. Basically this happens because zinc blende lacks an inversion center.²² Since the magnitude of $M_{\mu\nu}$ is proportional to the spin-orbit interaction, one might expect that the “forbidden” transition to s states might be small. This is in accord with the small intensity of the bound states relative to the continuum.

CdS: The two-photon spectrum of CdS was measured by Regensburger and Panizza.⁴ CdS has the wurtzite structure, and optical selection rules differ according to whether the polarization vectors are oriented parallel or perpendicular to the C axis. They had the Nd laser directed along the C axis. The probe beam was directed perpendicular to the C axis. The dichroism they observed could be caused by either the dichroism of the CdS or the dichroism caused by interchanging the order in which the two photons are absorbed. The interesting peaks in the spectrum are partly caused by the separate contributions from the three valence bands. Further polarizations studies are needed before this complex spectrum can be unraveled.

TlCl: Matsuoka³ has reported extensive two-photon measurements in TlCl. This material has the CsCl structure and its group-theoretical selection rules are the same as in alkali halides. The two-photon spectrum rises linearly with frequency, in agreement with the expectation for p -state exciton absorption. Matsuoka also measured the polarization dependence and discussed his results theoretically. He deduced that the polarization should obey a $\cos^2\theta = (\hat{\epsilon}_1 \cdot \hat{\epsilon}_2)^2$ law, but did not derive an equation analogous to (2.17). The angular dependence he observed did have the type of $\cos^2\theta$ behavior indicated by (2.17). However, his data contain two features which can not be explained by (2.17): (1) Although his data show that the absorption is maximum when $\hat{\epsilon}_1 \parallel \hat{\epsilon}_2$ ($\cos^2\theta=1$) and minimum when $\hat{\epsilon}_1 \perp \hat{\epsilon}_2$ ($\sin^2\theta=1$), the ratio of the minimum to the maximum absorption depended upon the orientation of $\hat{\epsilon}_1$

²³ In analyzing the group theory for these transitions in zinc-blende (T_d) we decided that (Γ_5 of Fröhlich) = (Γ_4 of Dresselhaus) = (Γ_{15} of Parmenter) = (T_2 of Heine, and also of Inoue and Toyozawa). We have adopted Inoue and Toyozawa's notation. This confusion has apparently arisen because this representation transforms like *both* sets of basis vectors (x, y, z) and (yz, zx, xy), whereas in O_h these basis sets belong to T_1 and T_2 , respectively.

²⁴ M. Cardona, Phys. Rev. **129**, 69 (1963).

and ϵ_2 with regard to the crystal axes. This feature is not predicted by our results for p -wave absorption, although the s - and d -wave absorptions, forbidden in this case, do depend upon the orientation with respect to crystal axes. (2) The ratio of the minimum to the maximum absorption was in some cases less than one-half. The present calculation predicts that this ratio is given by (4.1) and the algebraic form of R in (4.1) limits it to values between $\frac{1}{2}$ and 1 for any values of the $J_p(k)$'s. Thus we cannot explain these features of Matsuoka's data. We also considered whether the harmonic generation effects discussed by Jha were important. However, Jha points out that his additional absorption processes were unimportant in crystals with inversion symmetry, and therefore should not be relevant in the present case.²⁵

ACKNOWLEDGMENTS

I wish to thank Professor J. J. Hopfield for originally suggesting this problem to me. Professor Hopfield was the first to realize that a two-band model was adequate to solve the problem. My understanding of the physics was considerably improved through many conversations with Dr. J. D. Kingsley.

APPENDIX I: INTEGRAL EVALUATION

Here we summarize some of the ways we have found to express and evaluate the integrals which are encountered in this calculation. The result will be given only for the bound p -state integral $J_{p,n}$, but similar comments apply to all of the other integrals. Our original hope was that these integrals could be reduced to a single series. We finally concluded that this was impossible, and the reasons for this pessimism are provided below.

Single series can always be expressed in terms of hypergeometric functions. Similarly, there exist some standard definitions of double series which are natural extensions of the single-series hypergeometric functions.²⁶ For the present discussion, we need the following definitions and relations²⁶

$$F_1(\alpha, \beta, \beta', \gamma, x, y) = \sum_{m,n=0}^{\infty} \frac{(\alpha)_{m+n} (\beta)_m (\beta')_n}{(\gamma)_{m+n} m! n!} x^m y^n, \quad (\text{AI1})$$

$$F_3(\alpha, \alpha', \beta, \beta', \gamma, x, y) = \sum_{m,n=0}^{\infty} \frac{(\alpha)_m (\alpha')_n (\beta)_m (\beta')_n}{(\gamma)_{m+n} m! n!} x^m y^n, \quad (\text{AI2})$$

$$F_3(\alpha, \alpha', \beta, \beta', \gamma = \alpha + \alpha', x, y) = [1/(1-y)^{\beta'}] \times F_1[\alpha, \beta, \beta', \alpha + \alpha', x, -y/(1-y)], \quad (\text{AI3})$$

²⁵ S. S. Jha, Phys. Rev. 145, 500 (1966).

²⁶ Higher Transcendental Functions, edited by A. Erdelyi (McGraw-Hill Book Co., New York, 1953), Vol. 1, Secs. 5.7 and 5.8.

$$\int_0^1 du u^{\alpha-1} (1-u)^{\gamma-\alpha-1} (1-ux)^{-\beta} (1-uy)^{-\beta'} = \frac{\Gamma(\alpha)\Gamma(\gamma-\alpha)}{\Gamma(\gamma)} F_1(\alpha, \beta, \beta', \gamma, x, y). \quad (\text{AI4})$$

If we examine the series definition (2.15) for $J_{p,n}$ we see that the terms are just given by an F_3 type of series in (AI2).

$$J_{p,n}(\kappa) = \frac{\kappa^2 \Gamma(1-\kappa)}{2t_0^{2+\kappa}} \times \left\{ \frac{1}{\Gamma(3-\kappa)} F_3\left(1-\kappa, 2, -\kappa, 2-n, 3-\kappa, 1-t_0, \frac{\kappa}{t_0 n}\right) - \frac{\kappa}{n t_0} \frac{1}{\Gamma(4-\kappa)} F_3\left(1-\kappa, 3, -\kappa, 2-n, 4-\kappa, 1-t_0, \frac{\kappa}{t_0 n}\right) \right\}.$$

These F_3 functions have the characteristic that $\alpha + \alpha' = \gamma$, so one can relate them to a F_1 by using (AI3). Furthermore, by using an additional Euler transformation among the F_1 functions,²⁶ this can be written

$$J_{p,n}(\kappa) = \frac{1}{2} [\kappa^2 \Gamma(1-\kappa)] \{ [1/\Gamma(3-\kappa)] \times F_1(2, n+1, 2-n, 3-\kappa, 1-t_0, t_0) - [\kappa/n \Gamma(4-\kappa)] \times F_1(3, n+2, 2-n, 4-\kappa, 1-t_0, t_0) \}. \quad (\text{AI5})$$

Our basic integrals such as $J_{p,n}$ can be expressed compactly as standard series, either of the type F_3 or, alternatively, as F_1 . This explains our pessimistic conclusion that it was impossible to reduce these further to obtain simple series. Mathematicians have constructed these standard double series because of the impossibility of reducing them further. The F_1 form was not used for numerical computation because for large values of the n -quantum number it does not converge very rapidly.

One may also use the integral definition (AI4) to obtain (AI5) directly. First we rewrite the basic integral (2.14) as

$$J_{p,n}(\kappa) = \frac{\kappa^2}{2} \int_0^{\infty} dt \left(\frac{1+t}{t} \right)^{\kappa} \left[t + \frac{1}{2} - \frac{\kappa}{2n} \right]^{n-2} \times \left[\frac{1}{(\ell+t_0)^{n+1}} - \frac{\kappa}{2n} \frac{1}{(\ell+t_0)^{n+2}} \right]. \quad (\text{AI6})$$

If we now make the variable change $u = (1+t)^{-1}$, we just get integrals of the type (AI4). This leads directly to the result (AI5).

Finally, we had promised a short derivation of the double series (2.15). This can be done by using the

binomial expansion for

$$\left[t + \frac{1}{2} - \frac{\kappa}{2n} \right]^{n-2} = \sum_{l=0}^{n-2} \frac{(2-n)_l}{l!} \binom{\kappa}{n}^l (t+t_0)^{n-2-l}.$$

When we use this expansion in (AI6), the integrand becomes a power series in $(t+t_0)^{-l}$. Integrating each term in the series yields (2.15).

APPENDIX II: POLARIZATION DEPENDENCE

Inoue and Toyozawa¹⁰ calculated the dependence of the s -state absorption upon the polarization $\hat{\epsilon}_1$ and $\hat{\epsilon}_2$ of the two optical beams. In Eqs. (3.31)–(3.34) we summarized their results for cubic crystals (O_h) and our results for d states. Here we will show how the calculation is done by outlining the steps for one of them, the T_2 state.

Essentially, one evaluates the matrix element for each distant final state, squares the matrix element, and sums over all final states. This seems incorrect for the exciton continuum states, where one might sum over final states before squaring. However, as is shown below, the two methods are equivalent.

The T_2 state is threefold degenerate, and we label these states x , y , and z . Each of these three is a permissible final state. For the z state, the \mathbf{M} tensor has the form $M_{xy}^{(z)}(T_2) = M_{yx}^{(z)}(T_2)$ and other components vanish. For the z state of T_2 we get

$$\epsilon_{\alpha\mu} M_{\mu\nu}^{(z)} \frac{\partial}{\partial x_{\nu'}} \epsilon_{\beta\lambda} \frac{\partial}{\partial x_{\lambda}} = M_{xy}^{(z)}(T_2) \times \left[l_{\alpha} m_{\beta} \frac{\partial^2}{\partial y \partial y'} + m_{\alpha} l_{\beta} \frac{\partial^2}{\partial x \partial x'} + l_{\alpha} l_{\beta} \frac{\partial^2}{\partial x \partial y'} + m_{\alpha} m_{\beta} \frac{\partial^2}{\partial y \partial x'} + n_{\beta} l_{\alpha} \frac{\partial^2}{\partial y' \partial z} + n_{\beta} m_{\alpha} \frac{\partial^2}{\partial x' \partial z} \right]. \quad (\text{AII1})$$

A similar result is obtained for the x and y states by permuting indices. The derivatives with respect to primed and unprimed variables act upon $G(\mathbf{r}, \mathbf{r}')$ as $\mathbf{r}' \rightarrow 0$. Let us now consider how the operator (AII1) is evaluated for an exciton continuum state. We wish to evaluate (3.5) for the final-state wave function (2.20). An operator of the type $\partial^2/\partial x \partial y$ creates an exciton state with the symmetry $Y_{2,xy}$ in (3.6). When one

integrates in (3.5), the result is proportional to $k_x k_y J_{p,k}(\kappa)$; the $k_x k_y$ factors comes from the angular integral of $P_2(\cos\omega) Y_{2xy}$, and the r integral gives $J_{p,k}$. If we use the spherical coordinates of $\mathbf{k} = (k, \theta_0, \varphi_0)$, this term may be written as $Y_{2,xy}(\theta_0, \varphi_0) J_{p,k}(\kappa)$. Similarly, the derivatives of the type $\partial^2/\partial x^2$ give exciton states of symmetry Y_0 , $Y_{2,0}$, and $Y_{2,\alpha}$. The integration over d^3r in (3.6) gives terms proportional to $Y_0(\theta_0, \varphi_0) J_{s,k}$ and $Y_{2,0}(\theta_0, \varphi_0) J_{d,k}$ and $Y_{2,\alpha}(\theta_0, \varphi_0) J_{d,k}$. The total results of putting (AII1) in (3.5) is

$$I_k^{(z)}(\alpha, \beta) = \frac{M_{xy}^{(z)} \bar{\mu} e^{-\eta\pi/2} 4}{\sqrt{V} 3} \sqrt{4\pi} \times \left\{ J_{s,k} Y_0 |\Gamma(1-i\eta)| (l_{\alpha} m_{\beta} + m_{\alpha} l_{\beta}) + J_{d,k} \frac{|\Gamma(3-i\eta)|}{\eta^2} \sqrt{15} \left[\frac{1}{\sqrt{3}} Y_{2,0} (l_{\alpha} m_{\beta} + m_{\alpha} l_{\beta}) - Y_{2,\alpha} (m_{\alpha} l_{\beta} - l_{\alpha} m_{\beta}) - Y_{2,xy} (l_{\alpha} l_{\beta} + m_{\alpha} m_{\beta}) - n_{\beta} l_{\alpha} Y_{2,yz} - n_{\beta} m_{\alpha} Y_{2,xz} \right] \right\}. \quad (\text{AII2})$$

The functions Y_0 , $Y_{2,0}$, etc. refer to (θ_0, φ_0) . A similar equation results when evaluating $I^{(x)}$ and $I^{(y)}$. These latter two can *not* be obtained by permuting indices in (AII2), because x^2 , y^2 , and z^2 contain different combinations of $Y_{2,0}$ and $Y_{2,\alpha}$. In order to evaluate the absorption coefficient, we must square (AII2) and average over angles $d\Omega_k$. Since the angular functions Y_0 , $Y_{2,0}$, etc., are orthogonal, one gets results equivalent to squaring them separately. In effect, there are eighteen different final states—six angular functions Y_0 , $Y_{2,0}$, etc., for each of the three states (x, y, z) of T_2 .

An additional complication arises because there are two terms in (2.2). These arise because the photons can be absorbed in either order. For each of the eighteen states, one must add these two terms before squaring. For example, the last term in (AII2) gives an absorption coefficient proportional to

$$|m_1 n_2 J_{d,k}(\kappa_1) + m_2 n_1 J_{d,k}(\kappa_2)|^2.$$

After summing up all of these contributions, one gets the result in (3.36).